Statin-induced GGPP depletion blocks macropinocytosis and starves cells with oncogenic defects

Zhihua Jiao[a], Huaqing Cai[b,1], Yu Long[a], Orit Katarina Sirka[a], Veena Padmanaban[a], Andrew J. Ewald[a], and Peter N. Devreotes[a,1]

[a]Department of Cell Biology, School of Medicine, Johns Hopkins University, Baltimore, MD 21205; and [b]National Laboratory of Biomacromolecules, Chinese Academy of Sciences Center for Excellence in Biomacromolecules, Institute of Biophysics, Chinese Academy of Sciences, 100101 Beijing, China

Contributed by Peter N. Devreotes, December 28, 2019 (sent for review October 14, 2019; reviewed by Richard H. Gomer and Joel A. Swanson)

Cancer cells display novel characteristics which can be exploited for therapeutic advantage. Isolated studies have shown that 1) the mevalonate pathway and 2) increased macropinocytosis are important in tumorigenesis, but a connection between these two observations has not been envisioned. A library screen for compounds that selectively killed *Dictyostelium pten*$^-$ cells identified pitavastatin. Pitavastatin also killed human breast epithelial MCF10A cells lacking PTEN or expressing K-Ras^{G12V}, as well as mouse tumor organoids. The selective killing of cells with oncogenic defects was traced to GGPP (geranylgeranyl diphosphate) depletion. Disruption of GGPP synthase in *Dictyostelium* revealed that GGPP is needed for pseudopod extension and macropinocytosis. Fluid-phase uptake through macropinocytosis is lower in PTEN-deleted cells and, as reported previously, higher in cells expressing activated Ras. Nevertheless, uptake was more sensitive to pitavastatin in cells with either of these oncogenic mutations than in wild-type cells. Loading the residual macropinosomes after pitavastatin with high concentrations of protein mitigated the cell death, indicating that defective macropinocytosis leads to amino acid starvation. Our studies suggest that the dependence of cancer cells on the mevalonate pathway is due to the role of GGPP in macropinocytosis and the reliance of these cells on macropinocytosis for nutrient uptake. Thus, inhibition of the networks mediating these processes is likely to be effective in cancer intervention.

cancer | chemotaxis | mevalonate pathway | small GTPases | tumor organoids

In cancer cells, oncogenes and tumor suppressors such as Rap/Ras, PI3K, and PTEN affect not only growth and survival but also cell morphology and migration (1, 2). Similarly, studies of cell migration in *Dictyostelium* have revealed that networks involving these proteins control cytoskeletal activity, pseudopod extension, and macropinocytosis (3, 4). Growth and migration pathways are often considered separate branches of these networks; instead, it is likely that growth depends critically on dynamic morphological changes involved in processes such as migration and nutrient uptake.

In migrating cells, there is exquisite spatiotemporal regulation of these networks. In *Dictyostelium*, coordinated waves of Ras and PI3K activation, and PTEN dissociation, propagate along the cell cortex, triggering cytoskeleton-dependent protrusions and contractions (5, 6). The traveling waves derive from the excitable nature of the signal transduction network (7). Perturbations equivalent to oncogenic mutations alter the wave properties, causing cells to display wider or longer, narrower protrusions (4, 8). Human cancer cell lines also display altered morphology and migratory behavior which can be traced to network excitability (9, 10).

Motivated by the remarkable conservation of these signal transduction networks, we reasoned that drugs that would kill *Dictyostelium* cells carrying "oncogenic" mutations would target cancer cells. This model organism is ideal for large-scale screens as it grows quickly at room temperature in inexpensive media and genetic screens have uncovered many genes with homologs later found to control the same cell biological processes in mammalian cells. We screened *Dictyostelium* wild-type and *pten*$^-$ cells and identified a number of compounds that selectively killed the mutant cells. We tested the most promising leads on human MCF10A *PTEN*$^{-/-}$ cells as well as a variety of mouse mammary tumor models.

Among the compounds that killed *Dictyostelium* and human cells lacking PTEN were several statins. Used widely to reduce cholesterol, statins have also been investigated in a variety of tumor cell lines and in several clinical trials (11–16). Some studies have suggested statins inhibit proliferation and differentiation of tumor cells (17–19). Others have suggested that statins target cancer cells by blocking protein geranylgeranylation (20), although the processes requiring these modifications are still unclear.

Independent studies have shown that macropinocytosis can serve as an important source of amino acids through protein uptake (21, 22). *Dictyostelium* and mammalian cells with increased Ras activity have increased macropinocytosis (21, 23). The additional amino acids derived from protein taken up by macropinocytosis can be used for protein synthesis and energy production (21). Some cancer cells and tumor tissues require more amino acids than typically available in the medium and deprivation of glutamine has been demonstrated compared with adjacent normal tissue (24, 25). Therefore, macropinocytosis seems to be more important for cancer cells than normal cells.

In this study, we show that statins selectively kill PTEN-deleted *Dictyostelium* and mammalian cells with oncogenic defects by inhibiting the mevalonate pathway, leading to GGPP (geranylgeranyl diphosphate) depletion. The depletion reduces macropinocytosis because the process requires an excitable signal

Significance

Our studies establish a connection between two isolated observations that 1) statins, taken by millions to lower cholesterol, have antitumor activity and 2) Ras-induced macropinocytosis is important in tumorigenesis. We discover that by depleting GGPP required for pseudopod extension and macropinocytosis, statins selectively kill cells with oncogenic defects by limiting nutrient uptake.

Author contributions: A.J.E. and P.N.D. designed research; Z.J., H.C., Y.L., O.K.S., and V.P. performed research; Z.J., H.C., and O.K.S. analyzed data; Z.J. and P.N.D. wrote the paper; and all authors revised the manuscript.

Reviewers: R.H.G., Texas A&M University; and J.A.S., University of Michigan.

The authors declare no competing interest.

[1]To whom correspondence may be addressed. Email: huaqingcai@ibp.ac.cn or pnd@jhmi.edu.

This article contains supporting information online at https://www.pnas.org/lookup/suppl/doi:10.1073/pnas.1917938117/-/DCSupplemental.

First published February 12, 2020.

transduction network containing multiple small GTPase proteins which must be geranylgeranylated. PTEN is involved in the same network. Mutations in these pathways alter migration and macropinocytosis and make these processes more sensitive to GGPP depletion. The loss of macropinocytosis finally leads to amino acid starvation and cell death. Thus, by demonstrating GGPP is required for macropinocytosis, we coupled the mevalonate pathway to the supply of nutrients for tumor cells and provide a mechanistic explanation for the effects of statins on cancer cells.

Results

Cells Lacking PTEN Are Selectively Sensitive to Statins. Aiming to identify drugs that kill cancer cells and spare normal cells, we performed a high-content screening of a library containing Food and Drug Administration (FDA)-approved drugs as well as those in clinical trials with *Dictyostelium* wild-type (WT) and *pten*$^-$ cells. Cell viability and morphology were monitored 48 and 72 h after drug administration (Fig. 1*A*). The effects of potential hits were confirmed with commercially purchased chemicals. Among the 2,560 tested drug compounds, seven altered cell growth or cell polarity in *pten*$^-$ cells (*SI Appendix*, Fig. S1). Surprisingly, drugs that most effectively and selectively targeted *pten*$^-$ cells were two statins, fluvastatin and pitavastatin. The results were further confirmed by testing seven commercially available statins. Pitavastatin and fluvastatin showed the best performance, as shown in Fig. 1 *B–D* and *SI Appendix*, Fig. S2. Simvastatin showed an intermediate effect, while the other four statins showed no or a slight effect on the cell viability of both WT and *pten*$^-$ cells. Compared with fluvastatin, pitavastatin was effective at 5- to 10-fold lower concentrations. Expression of PTEN-GFP in *pten*$^-$ cells restored cell viability to that of WT cells (Fig. 1*E*), demonstrating that the sensitivity to pitavastatin and fluvastatin was due to the deletion of PTEN.

To assess whether the cytotoxic effects of statins carry over to mammalian cells, the effects of seven statins on human breast epithelial MCF10A and corresponding *PTEN*$^{-/-}$ cells were tested. As shown in Fig. 1 *F–H*, *SI Appendix*, Fig. S3*A*, and Movie S1, pitavastatin killed *PTEN*$^{-/-}$ cells but had little effect on MCF10A cells at the same concentrations. Time-lapse videos showed that the pitavastain-treated *PTEN*$^{-/-}$ cells initially became spindle-shaped and then underwent apoptosis by 48 to 72 h (Movie S1). Similar results were obtained with fluvastatin but at a higher concentration (*SI Appendix*, Fig. S3*B*). Expressing PTEN in *PTEN*$^{-/-}$ cells restored the sensitivity of *PTEN*$^{-/-}$ cells to that of MCF10A cells (Fig. 1*I*). Therefore, the effects of statins on human *PTEN*$^{-/-}$ and *Dictyostelium pten*$^-$ cells are consistent.

We next tested the effects of pitavastatin on MCF10A and *PTEN*$^{-/-}$ cells in 3D (three-dimensional) culture. As shown in Fig. 2 *A–C*, wild-type spheroids were unaffected by pitavastatin at concentrations up to 2 μM. In contrast, with *PTEN*$^{-/-}$ cells, we observed a few broken spheroids with 0.5 μM. With higher doses of pitavastatin (1 or 2 μM), most of the spheroids were disrupted. Staining with fluorescein diacetate and propidium iodide indicated that, except for a few internal cells, most of the cells in the broken spheroids were dead. Expressing PTEN in *PTEN*$^{-/-}$ cells mitigated the sensitivity to pitavastatin (Fig. 2*D*). Taken together, pitavastatin is cytotoxic to not only *Dictyostelium pten*$^-$ cells but also human *PTEN*$^{-/-}$ cells in both 2D and 3D culture.

The Effects of Statins Are Mediated by GGPP Depletion. Statins act by inhibiting HMG-CoA reductase, which catalyzes the synthesis of mevalonic acid (Mev) (26) (Fig. 3*A*). To assess whether the

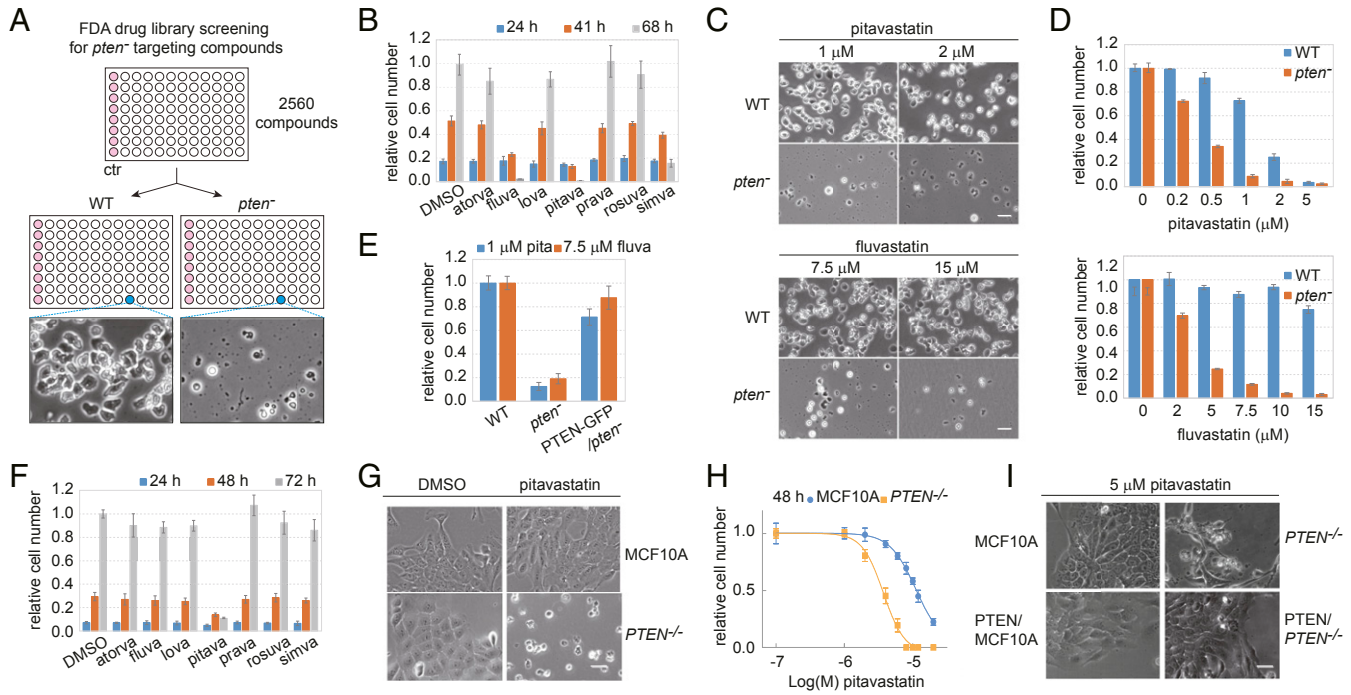

Fig. 1. Identification of *Dictyostelium* and mammalian *PTEN*$^{-/-}$ vulnerability to statins. (*A*) Schematic representation of the screening strategy. (*B*) Measurement of the growth of *pten*$^-$ cells in response to seven different statins (5 μM, mean ± SD, $n = 3$). (*C*) Cytotoxic effects of fluvastatin and pitavastatin on *Dictyostelium pten*$^-$ cells compared with WT. (Scale bars, 20 μm.) (*D*) Measurement of the growth of WT and *pten*$^-$ cells in response to increasing concentrations of fluvastatin or pitavastatin (mean ± SD, $n = 3$). (*E*) The expression of PTEN-GFP in *pten*$^-$ cells renders resistance to fluvastatin and pitavastatin (mean ± SD, $n = 3$). (*F*) Measurement of the growth of *PTEN*$^{-/-}$ cells in response to seven different statins (5 μM, mean ± SD, $n = 3$). (*G*) Cytotoxic effects of pitavastatin (5 μM) on mammalian *PTEN*$^{-/-}$ cells compared with MCF10A and dimethyl sulfoxide (DMSO) control. (Scale bar, 30 μm.) (*H*) Measurement of the growth of MCF10A and *PTEN*$^{-/-}$ cells in response to increasing concentrations of pitavastatin (mean ± SD, $n = 3$). (*I*) The expression of PTEN in *PTEN*$^{-/-}$ cells renders resistance to pitavastatin. (Scale bar, 30 μm.)

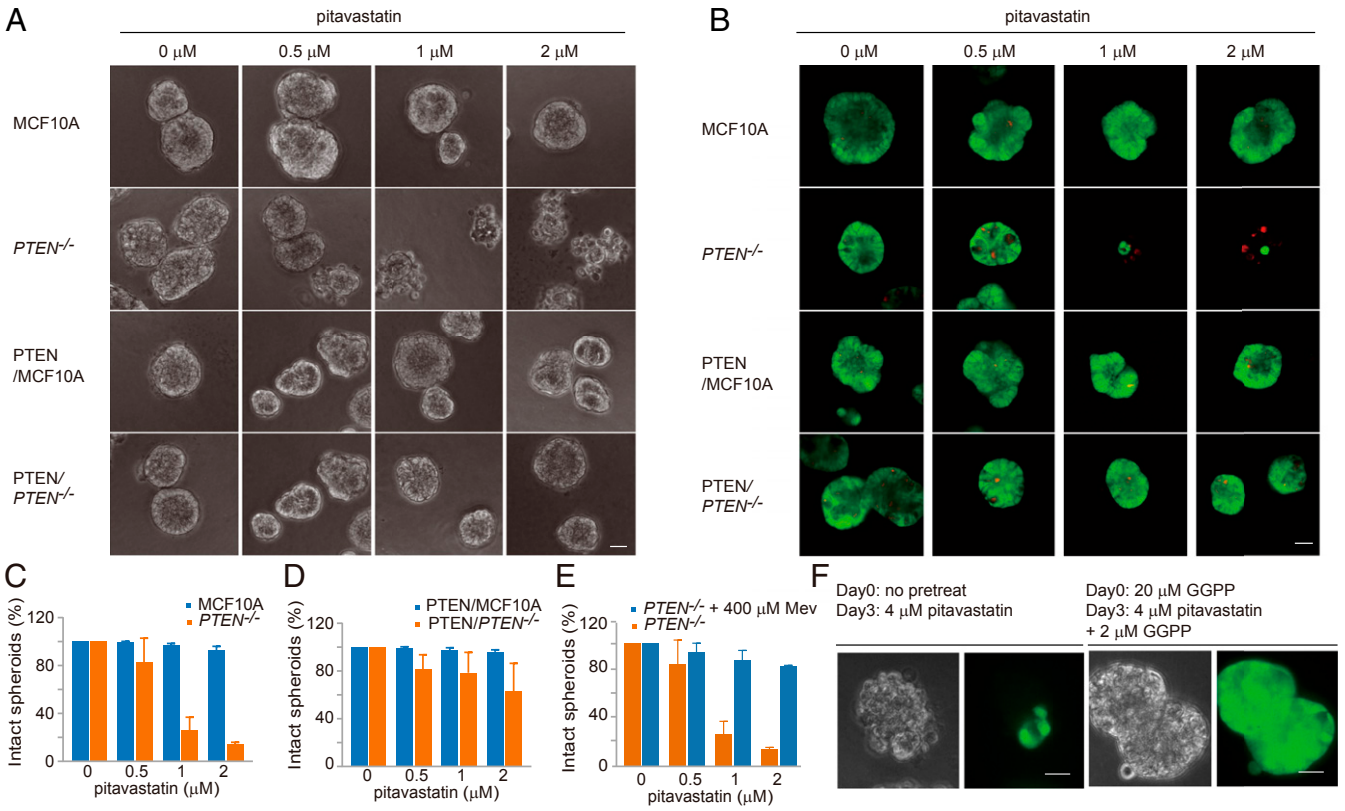

Fig. 2. *PTEN*$^{-/-}$ spheroids are vulnerable to perturbation of the mevalonate pathway. (*A*) Cytotoxic effects of pitavastatin on MCF10A and *PTEN*$^{-/-}$ spheroids in 3D culture. (Scale bar, 30 μm.) (*B*) MCF10A and *PTEN*$^{-/-}$ spheroid staining with fluorescein diacetate and propidium iodide after pitavastatin treatment. (Scale bar, 30 μm.) (*C*) Measurement of the intact spheroids of MCF10A and *PTEN*$^{-/-}$ in response to increasing concentrations of pitavastatin (mean ± SD, n = 500 spheroids). (*D*) Measurement of the intact spheroids of PTEN/MCF10A and PTEN/*PTEN*$^{-/-}$ in response to increasing concentrations of pitavastatin (mean ± SD, n = 500 spheroids). (*E*) Measurement of the intact spheroids of *PTEN*$^{-/-}$ in the absence or presence of Mev and increasing concentrations of pitavastatin (mean ± SD, n = 500 spheroids). (*F*) The addition of GGPP rescues pitavastatin-induced cell death of *PTEN*$^{-/-}$ in 3D culture. (Scale bars, 30 μm.)

cytotoxic effects of pitavastatin are via the mevalonate pathway, we performed add-back experiments in *PTEN*$^{-/-}$ cells treated with pitavastatin. As shown in Fig. 3 *B–D*, addition of Mev completely prevented the cytotoxic effects of pitavastatin in both *Dictyostelium pten*$^{-}$ and MCF10A *PTEN*$^{-/-}$ cells.

To examine whether the cytotoxic effects of pitavastatin were due to decreased production of cholesterol or other intermediate metabolites of the mevalonate pathway (Fig. 3*A*), we tested three inhibitors that target distinct reactions. YM-53601 inhibits squalene synthase, which should lower cholesterol production (27). FTI-277 blocks protein farnesylation by inhibiting farnesyl transferase (28). GGTI-298 blocks protein geranylgeranylation via inhibition of geranylgeranyl transferase (29). As shown in Fig. 3*E*, inhibition of squalene synthase or farnesyl transferase had little effect on *PTEN*$^{-/-}$ cells, whereas GGTI-298 altered the morphology of *PTEN*$^{-/-}$ cells similar to the early effects of pitavastatin. However, the effects were transient.

To further test that the cytotoxic effects of pitavastatin are due to GGPP depletion, we added back geranyl pyrophosphate (GPP) or GGPP. Supplementation with GPP or GGPP completely abrogated the effects of pitavastatin in PTEN-deleted cells (Fig. 3 *B*, *F*, and *G*). Moreover, the effects of pitavastatin in 3D *PTEN*$^{-/-}$ spheroids were also traced to GGPP depletion since supplementation with mevalonic acid or GGPP could completely eliminate the cytotoxic effects of pitavastatin (Fig. 2 *E* and *F*).

To demonstrate that pitavastatin at the effective doses altered protein prenylation, we assessed the electrophoretic mobility and expression levels of multiple Rab and Rho family proteins with predicted geranylgeranylation. As shown in *SI Appendix*, Fig. S4 *A–C*, the mobility of Rab5, Rab7, and Rab11 decreased with pitavastatin treatment. We surmised that the decreased mobility was due to loss of the lipid modification. Interestingly, RhoA levels were significantly induced by pitavastatin treatment and could be restored by the addition of GGPP (*SI Appendix*, Fig. S4 *C* and *D*). Perhaps this induction is a reaction to the loss of RhoA on the membrane. Using this induction as a readout, we found no difference in dose dependence in wild-type versus *PTEN*$^{-/-}$ cells.

GGPP Is Required for Robust Cell Motility and Macropinocytosis. Geranylgeranyl diphosphate synthase (GGPPS) generates GGPP from farnesyl diphosphate and isopentenyl diphosphate (30) (Fig. 3*A*). We deleted GGPPS in *Dictyostelium* cells and assessed whether its loss induced the same cytotoxic effects as pitavastatin. As shown in Fig. 4*A*, in the absence of GGPP, *ggps1*$^{-}$ cells die in 48 h, while with 0.2 μM GGPP, they grow at the same rate as wild-type cells. The cells could survive at concentrations as low as 30 nM as long as it was continuously supplied (*SI Appendix*, Fig. S5*A*). Expressing *Dictyostelium* or human GGPPS in *ggps1*$^{-}$ cells reversed the GGPP-dependent growth (Fig. 4*B* and *SI Appendix*, Fig. S5*B*). These results confirmed the requirement of GGPP for normal cell physiology.

We reasoned that overexpressing multiple predicted geranylgeranylated proteins in *Dictyostelium pten*$^{-}$ cells might partially suppress the effects of pitavastatin. Increasing the concentration of apoprotein when GGPP is partially reduced should increase the reaction rate and restore an adequate level of geranylgeranylated protein. Protein sequence analyses in *Dictyostelium* revealed predicted targets of GGTase-I with CAAL at the C terminus as RapA,

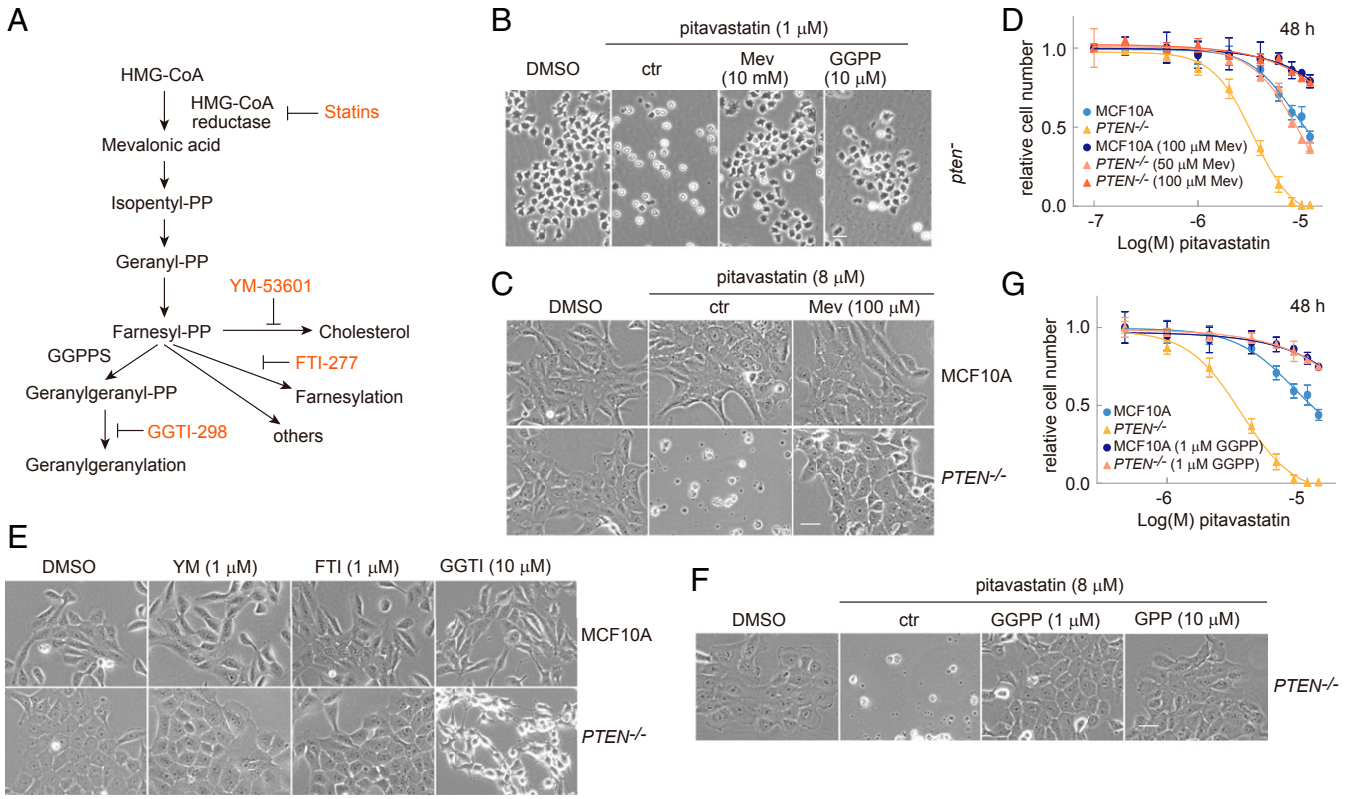

Fig. 3. Modulation of geranylgeranylation mediates the cytotoxic effects of pitavastatin. (*A*) Schematic of the mevalonate pathway. Chemical inhibitors of specific steps are in orange. (*B*) The addition of Mev or geranylgeranyl pyrophosphate (GGPP) rescues pitavastatin-induced cell death in *Dictyostelium pten*$^-$ cells. Images were taken 72 h after drug addition. (Scale bar, 20 μm.) (*C*) The addition of Mev rescues pitavastatin-induced cell death in MCF10A *PTEN*$^{-/-}$ cells. Images were taken 68 h after drug addition. (Scale bar, 30 μm.) (*D*) Measurement of MCF10A and *PTEN*$^{-/-}$ cell growth in the absence or presence of Mev and increasing concentrations of pitavastatin (mean ± SD, $n = 3$). (*E*) Inhibition of geranylgeranyl transferase (with GGTI, 48 h), but not squalene synthase (with YM, 68 h) or farnesyl transferase (with FTI, 68 h), is able to recapitulate pitavastatin treatment. (Scale bar, 30 μm.) (*F*) The addition of GGPP or geranyl pyrophosphate rescues pitavastatin-induced cell death. Images were taken 68 h after drug addition. (Scale bar, 30 μm.) (*G*) Measurement of MCF10A and *PTEN*$^{-/-}$ cell growth in the absence or presence of GGPP and increasing concentrations of pitavastatin (mean ± SD, $n = 3$).

RasB, RasC, RasD, RacE, RacL, RacM, and dhkH. There are an additional 48 putative targets of GGTase-II. Expression of these GGTase-I substrates singly had little effect; however, expressing RasB, RasC, RasD, RacL, RacM, and RapA simultaneously in *pten*$^-$ cells increased cell viability. Although pitavastatin killed a large fraction of cells in both cases, around five times more cells survived with expression of the six proteins (Fig. 4*C* and *SI Appendix*, Fig. S5*C*). This suggests that these proteins are among the important geranylgeranylated targets needed for cell survival.

We noticed that during GGPP depletion, the motility of *ggps1*$^-$ cells decreased gradually and eventually they stopped moving (Fig. 4 *D* and *E* and Movie S2). In addition, the *ggps1*$^-$ cells extended much smaller protrusions and appeared less polarized (Fig. 4*F* and Movie S3). Our previous studies showing that motility and macropinocytosis are closely related processes requiring the same excitable signal transduction network prompted us to examine whether GGPP was also required for fluid-phase uptake. As shown in Fig. 4 *G* and *H*, incubation with TRITC-dextran revealed strong defects in macropinocytosis in *ggps1*$^-$ cells. Adding back GGPP was sufficient to restore macropinocytosis. Taken together, these observations demonstrate that GGPP, perhaps through the small GTPases, is required for making protrusions that underlie optimal cell motility and macropinocytosis.

Macropinocytosis Is Defective and More Sensitive to GGPP Depletion in Cells Lacking PTEN. Since GGPP is required for macropinocytosis and pitavastatin depletes GGPP, we tested the effects of pitavastatin on fluid-phase uptake in both WT and *pten*$^-$ *Dictyostelium* cells. As shown in Fig. 5 *A* and *B*, we found that fluid-phase uptake in *pten*$^-$ cells was 66% lower than in wild-type cells, even in the absence of pitavastatin. Careful examination revealed that the macropinosomes in *pten*$^-$ cells were 40% smaller than those in wild-type cells (*SI Appendix*, Fig. S6 *B* and *C*), accounting for the reduced uptake. The smaller size was apparent at the earliest steps in the formation of the macropinosomes, visualized within 3 min with FM lipophilic styryl dye (Movie S4). Pitavastatin treatment further reduced uptake in *pten*$^-$ cells to nearly undetectable levels while it had little effect on wild-type cells (Fig. 5 *A* and *B* and *SI Appendix*, Fig. S6*A*).

We next examined whether the correlation between pitavastatin sensitivity and macropinocytosis seen in *Dictyostelium* cells extended to MCF10A wild-type and *PTEN*$^{-/-}$ cells. As shown in Fig. 5 *C* and *D*, macropinocytosis was 46% lower in *PTEN*$^{-/-}$ cells than in wild-type cells. The macropinosomes in *PTEN*$^{-/-}$ cells were fewer in number and less intense. Significantly, pitavastatin reduced macropinocytosis in *PTEN*$^{-/-}$ cells by an additional 41% while it only slightly decreased uptake in wild-type cells (*SI Appendix*, Fig. S6*D*).

The severe inhibition of macropinocytosis by pitavastatin in *Dictyostelium* and MCF10A cells lacking PTEN pointed to starvation as the mechanism of cell death. We examined the expression of the microtubule-associated protein light chain 3 (LC3), a widely used marker for autophagocytosis (31). As shown in Fig. 5*E* and *SI Appendix*, Fig. S6*E*, during treatment with a high dose of

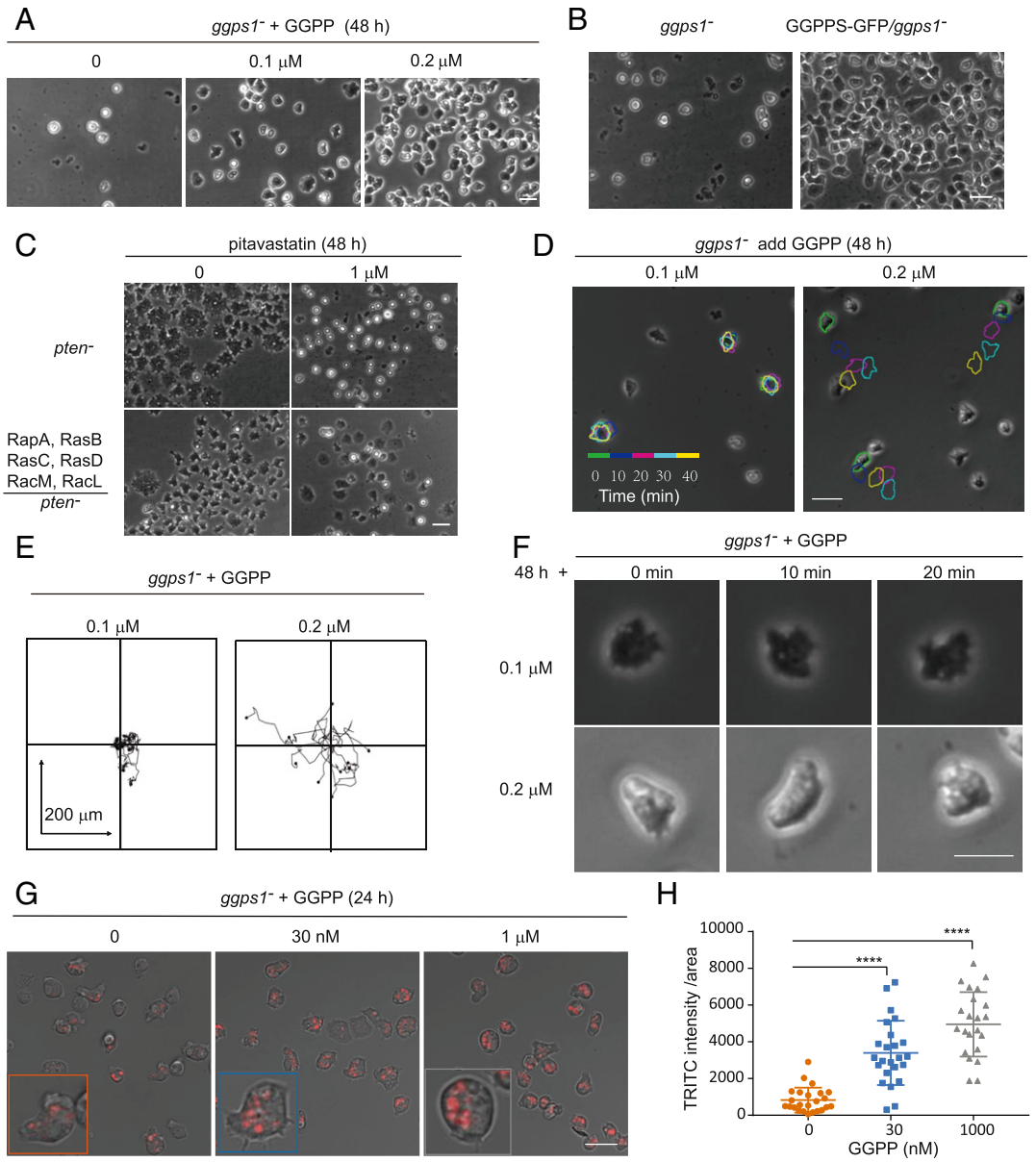

Fig. 4. GGPP is essential for cell migration and macropinocytosis. (*A*) *ggps1*$^{-}$ cells could not survive without addition of GGPP. (Scale bar, 20 μm.) (*B*) The expression of *Dictyostelium* GGPPS-GFP in *ggps1*$^{-}$ cells renders their survival independent of GGPP. (Scale bar, 20 μm.) (*C*) Overexpressing RapA, RasB, RasC, RasD, RacM, and RacL in *Dictyostelium pten*$^{-}$ cells partially suppresses the effects of pitavastatin. (Scale bar, 20 μm.) (*D*) Color-coded outlines (10 min apart) of several cells (*ggps1*$^{-}$ cells with 0.1 μM GGPP [*Left*] or 0.2 μM GGPP [*Right*] after 48 h) were imposed on top of the phase images, with yellow outlining the last cells. (Scale bar, 20 μm.) (*E*) Cell migration tracks showing random movement of cells from *D*. (*F*) Time-lapse phase-contrast images showing single cells from *D* and *E* at 10-min intervals indicating that GGPP is required for *Dictyostelium* cells to make protrusions. (Scale bar, 10 μm.) (*G*) The effects of GGPP on fluid-phase uptake in *Dictyostelium ggps1*$^{-}$ cells. (Scale bar, 20 μm.) (*H*) Measurement of fluid-phase uptake in *ggps1*$^{-}$ cells in the presence of increasing concentrations of GGPP ($n = 3$ experiments, one-way ANOVA with post hoc Tukey HSD (honestly significant difference) test, ****$P < 0.0001$).

pitavastatin, there was a larger increase of LC3-II in *PTEN*$^{-/-}$ cells compared with wild-type cells. These results suggest that dysregulation of macropinocytosis by pitavastatin in PTEN-deleted cells induces starvation.

Macropinocytosis Delivers Proteins and Amino Acids to Cells. Based on our observation that defects in macropinocytosis lead to cell starvation, we sought to determine the critical components being delivered to the cell through the macropinosomes. Since serum albumin is a major component in extracellular fluid taken up by macropinocytosis, we tested its role in the pitavastatin sensitivity in MCF10A cells. In serum-free medium, both wild-type and *PTEN*$^{-/-}$ cells were more sensitive to pitavastatin (compare Fig. 6*A* with Fig. 1 *G* and *H*). For example, in serum-free medium, *PTEN*$^{-/-}$ cells were selectively killed at 3 μM in 48 h, while in complete medium, they were killed at 5 μM in 72 h. Supplementation with BSA (bovine serum albumin) increased cell viability in both wild-type and *PTEN*$^{-/-}$ cells. For *PTEN*$^{-/-}$ cells, 0.5% BSA prevented the cell death, but restoration of normal morphology required 3% BSA (Fig. 6*B*).

To explore the mechanism of BSA rescue, we monitored fluid-phase uptake with Alexa BSA. As shown in Fig. 6*C* and *SI Appendix*, Fig. S7 *A* and *B*, with increasing concentrations of unlabeled BSA, the uptake of Alexa BSA was slightly reduced. However, the calculated amount of total BSA entering cells

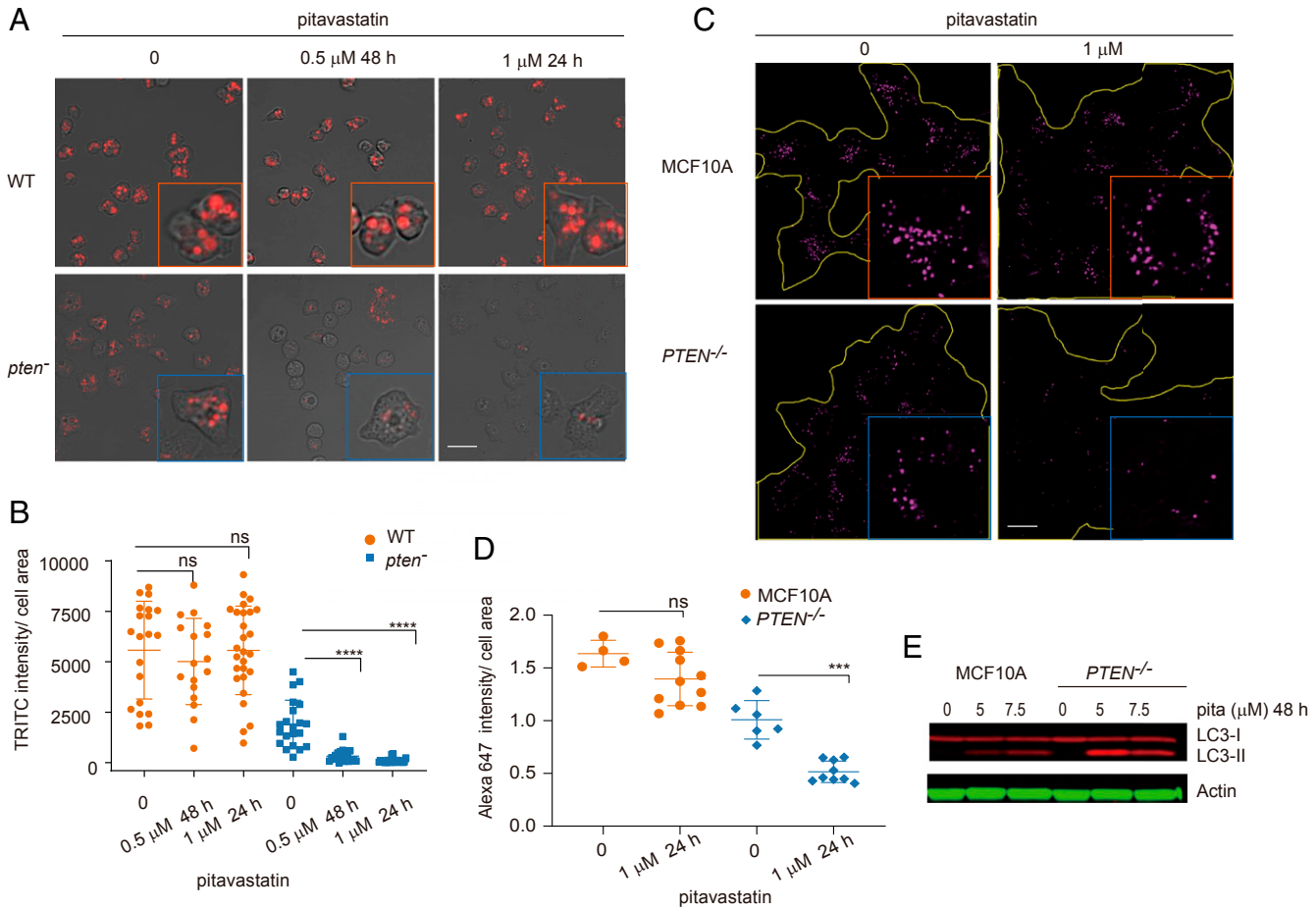

Fig. 5. Macropinocytosis in PTEN-deleted cells shows more defects and higher sensitivity to pitavastatin than wild-type cells. (*A*) The effects of pitavastatin on fluid-phase uptake in *Dictyostelium* wild-type and *pten*$^-$ cells. (Scale bar, 20 μm.) (*B*) Measurement of fluid-phase uptake in wild-type and *pten*$^-$ cells in the presence of increasing concentrations of pitavastatin ($n = 3$ experiments, one-way ANOVA with post hoc Tukey HSD test, ****$P < 0.0001$; ns, not significant). (*C*) The effects of pitavastatin on fluid-phase uptake in MCF10A and *PTEN*$^{-/-}$ cells. Groups of cells are outlined with yellow. (Scale bar, 20 μm.) (*D*) Measurement of fluid-phase uptake in MCF10A and *PTEN*$^{-/-}$ cells in the presence of increasing concentrations of pitavastatin. For each condition, 4 to 11 images are used for quantification, and each image includes 10 to 20 cells ($n = 3$ experiments, nonparametric Mann–Whitney–Wilcoxon test, ***$P < 0.001$). (*E*) *PTEN*$^{-/-}$ cells are more starved than MCF10A cells after pitavastatin treatment. MCF10A and *PTEN*$^{-/-}$ cells were treated with pitavastatin for the indicated period, and cell lysates were subjected to immunoblot analysis with an anti-LC3 antibody. The positions of LC3-I and LC3-II are indicated. The ratio of LC3-II to total LC3 indicates the level of cell starvation.

increased almost linearly. This suggests that the BSA did not increase the number or size of macropinosomes but filled the macropinosomes remaining after pitavastatin treatment with more protein. As leucine is the most abundant amino acid in BSA, we tested whether it also could mitigate the effect of pitavastatin. As shown in Fig. 6*D*, supplementation of serum-free medium with a 70-fold excess of leucine or a combination of leucine and excess essential amino acids also restored the viability.

We could not perform a completely parallel experiment in *Dictyostelium*; however, by switching media, we were able to replace the proteose peptone and yeast extract in HL5 medium with high concentrations of amino acids in FM medium. When cells were switched from HL5 to FM, macropinocytosis increased slightly in wild-type cells. In *pten*$^-$ cells, uptake was nearly as high as wild-type cells (Fig. 6 *E* and *F* and *SI Appendix*, Fig. S7 *C* and *D*). In both media, pitavastatin decreased macropinocytosis to some extent in wild-type cells, while the decrease was more significant in *pten*$^-$ cells (Fig. 6 *E* and *F* and *SI Appendix*, Fig. S7 *C* and *D*). However, the remaining uptake of *pten*$^-$ cells in FM medium after pitavastatin was still comparable to that in HL5 medium without pitavastatin. Apparently, this residual uptake in FM medium was sufficient to prevent the death of *pten*$^-$ cells even in 4 μM pitavastatin (Fig. 6*G* and *SI Appendix*, Fig. S7*E*). These results suggest cells only die when uptake drops below a critical level.

Macropinocytosis Is Elevated and More Sensitive to GGPP Depletion in Cells Expressing K-Ras^{G12V}. To test whether pitavastatin only selectively targets cells with defective macropinocytosis, such as PTEN-deleted cells, we also tested the effects of pitavastatin on K-Ras^{G12V}–expressing MCF10A cells. These cells are reported to have induced macropinocytosis. During the initial experiments, we realized that K-Ras^{G12V}–expressing MCF10A cells deplete nutrients faster than MCF10A wild-type cells and die sooner if media are not refreshed. We therefore tested pitavastatin sensitivity when K-Ras^{G12V}–expressing MCF10A cells and wild-type MCF10A cells were mixed together with GFP labeling the K-Ras^{G12V}–positive cells. In both complete medium and serum-free medium, K-Ras^{G12V}–positive cells were selectively sensitive to pitavastatin. As shown in Fig. 7 *A* and *B*, most of the dead cells after pitavastatin treatment are labeled with GFP. Supplementation of GGPP completely restored the sensitivity to that of wild-type cells (Fig. 7*C*), indicating the effects of pitavastatin on K-Ras^{G12V} cells are mediated by protein geranylgeranylation. As observed for *PTEN*$^{-/-}$ cells, the sensitivity is higher in serum-free medium, which requires

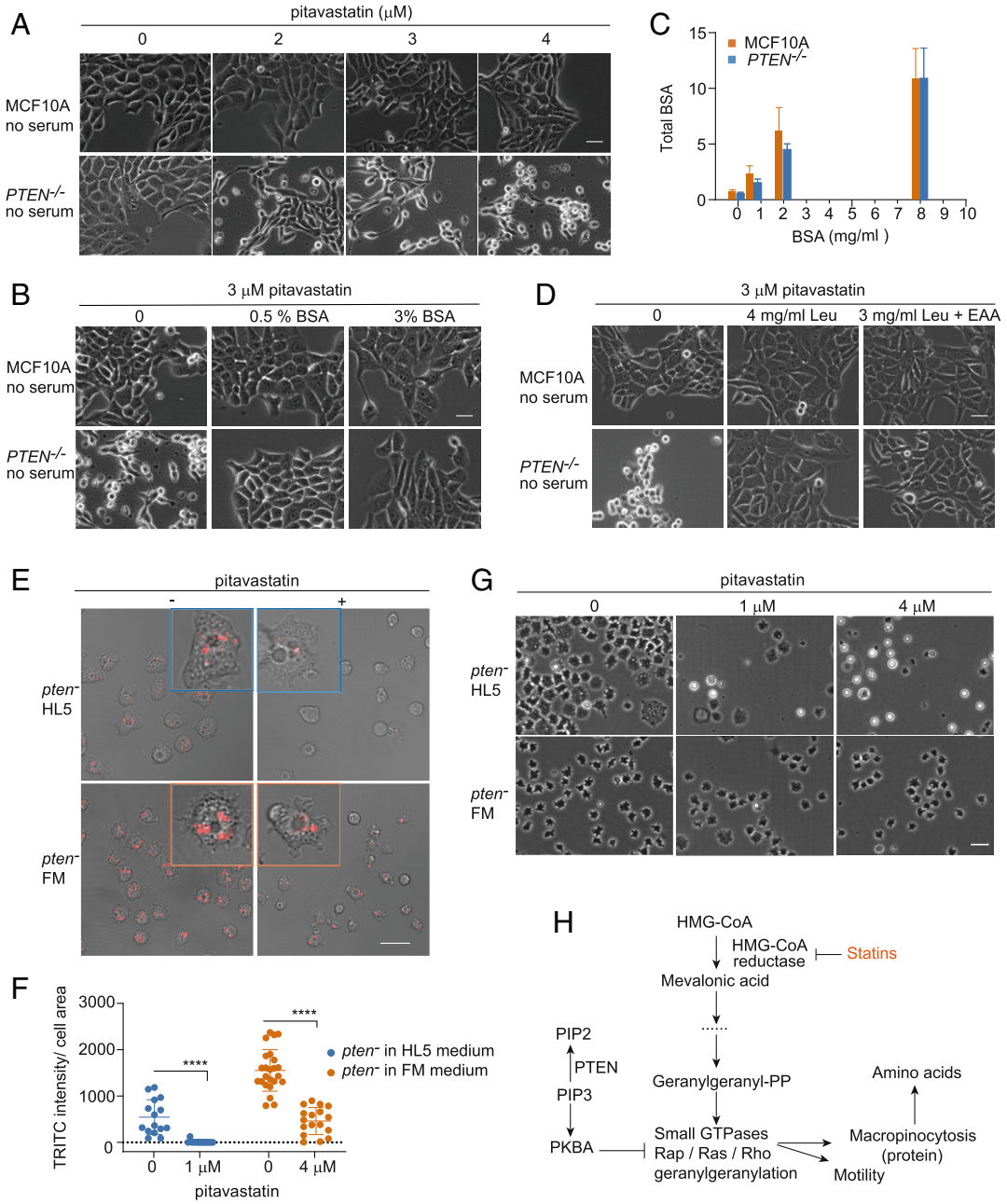

Fig. 6. Defective macropinocytosis after pitavastatin induces protein and amino acid starvation in *PTEN*$^{-/-}$ cells. (*A*) The sensitivity of pitavastatin increases in *PTEN*$^{-/-}$ cells under serum-free conditions. (Scale bar, 30 μm.) (*B*) BSA rescues the cytotoxic effects of pitavastatin in mammalian *PTEN*$^{-/-}$ cells under serum-free conditions. (Scale bar, 30 μm.) (*C*) Total intracellular BSA in MCF10A and *PTEN*$^{-/-}$ cells increases with increasing concentrations of BSA in the medium (mean ± SD, $n = 3$). (*D*) Leucine (Leu) rescues the cytotoxic effects of pitavastatin on mammalian *PTEN*$^{-/-}$ cells under serum-free conditions. (Scale bar, 30 μm.) (*E*) Fluid-phase uptake in *Dictyostelium pten*$^{-}$ cells in HL5 medium and FM medium. *pten*$^{-}$ cells in HL5 medium were added with 1 μM pitavastatin; *pten*$^{-}$ cells in FM medium were added with 4 μM pitavastatin. (Scale bar, 20 μm.) (*F*) Measurement of fluid-phase uptake in *Dictyostelium pten*$^{-}$ cells in HL5 medium and FM medium ($n = 3$ experiments, nonparametric Mann–Whitney–Wilcoxon test, ****$P < 0.0001$). (*G*) *Dictyostelium pten*$^{-}$ cells show resistance to pitavastatin in FM medium containing abundant amino acids. (Scale bar, 20 μm.) (*H*) Proposed molecular architecture of the mevalonate pathway and macropinocytosis.

a dose of only 2 μM compared with the 7 μM in complete medium (Fig. 7 *A* and *B*).

To address the extent to which pitavastatin inhibits induced macropinocytosis in K-Ras^{G12V}–expressing MCF10A cells, we performed the fluid-uptake experiments with K-Ras^{G12V}–positive and wild-type cells in the same well. Each cell is outlined for quantification of macropinocytosis; K-Ras^{G12V}–positive cells are defined based on their GFP intensity. As shown in Fig. 7 *D* and *E*, K-Ras^{G12V}–positive cells exhibit a 1.87-fold higher level of macropinocytosis per area than K-Ras^{G12V}–negative cells before pitavastatin treatment. Since K-Ras^{G12V}–expressing cells are generally larger in area, the total uptake of GFP-positive cells was 2.2-fold higher than GFP-negative cells. Following treatment with 1 μM pitavastatin, macropinocytosis decreased 11% in wild-type cells and 64% in K-Ras^{G12V}–positive cells. With 2 μM pitavastatin, macropinocytosis decreased 17% in wild-type cells and 84% in

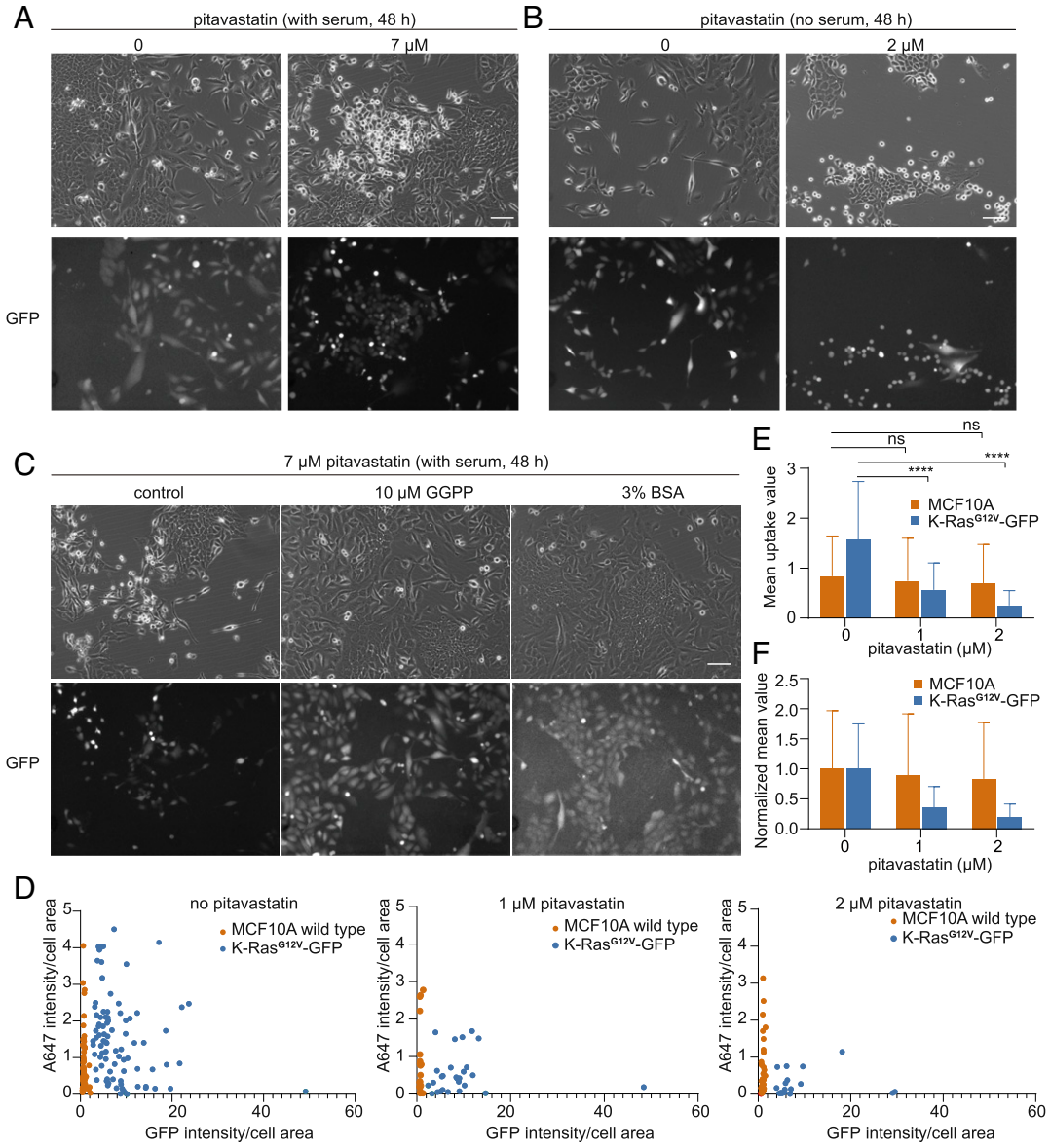

Fig. 7. MCF10A cells expressing K-Ras^{G12V}-GFP are vulnerable to perturbation of the mevalonate pathway. (*A*) Cytotoxic effects of pitavastatin on MCF10A cells expressing K-Ras^{G12V}-GFP compared with wild-type cells in complete medium. Both MCF10A wild-type cells and Ras^{G12V}-GFP cells are included in the bright-field image. Only K-Ras^{G12V}-GFP cells are labeled in GFP images. (Scale bar, 20 μm.) (*B*) Cytotoxic effects of pitavastatin on MCF10A cells expressing K-Ras^{G12V}-GFP compared with wild-type cells in serum-free medium. (Scale bar, 20 μm.) (*C*) Supplementation of GGPP and BSA rescues pitavastatin-induced cell death in K-Ras^{G12V}-GFP cells. (Scale bar, 20 μm.) (*D*) Measurement of fluid-phase uptake in MCF10A wild-type and K-Ras^{G12V}-GFP–expressing cells in the presence of increasing concentrations of pitavastatin. For each condition, a single cell is outlined for quantification; cells with less GFP signal are recognized as wild-type cells. (*E*) The mean value of fluid-phase uptake in MCF10A wild-type and K-Ras^{G12V}-GFP–expressing cells in the presence of increasing concentrations of pitavastatin (mean ± SD, $n = 3$ experiments, one-way ANOVA with post hoc Tukey HSD test, ****$P < 0.0001$). (*F*) The normalized mean value of fluid-phase uptake in MCF10A wild-type and K-Ras^{G12V}-GFP–expressing cells in the presence of increasing concentrations of pitavastatin (mean ± SD).

K-Ras^{G12V}–positive cells (Fig. 7*F*). Taken together, even though K-Ras^{G12V} cells display increased macropinocytosis compared with wild-type cells, these cells also display higher sensitivity to inhibition of macropinocytosis by pitavastatin.

To further confirm that K-Ras^{G12V} cells die after pitavastatin treatment due to starvation, we also assessed the effects of supplementation with high concentrations of BSA. Consistent with the effects of BSA on *PTEN*$^{-/-}$ MCF10A cells, K-Ras^{G12V} cells were also able to survive under treatment with pitavastatin and BSA together (Fig. 7*C*). In these experiments, excess BSA did not increase the uptake of fluorescent BSA, indicating that the rescue was due to increasing the protein content of the residual macropinosomes. These results demonstrate that pitavastatin targets both *PTEN*$^{-/-}$ and K-Ras^{G12V} cells by blocking the uptake of protein.

Mouse Tumor Organoid Models Are Vulnerable to Pitavastatin. Several studies have suggested that malignant cells are more highly dependent on the continuous availability of mevalonate pathway metabolites than normal cells, including breast cancer (26, 32). To investigate whether cytotoxic effects of pitavastatin are generalizable to other cancer models with mutations other than PTEN deletion and expressing K-Ras^{G12V}, we examined three different mouse models: *Twist1*-overexpressing mammary epithelial

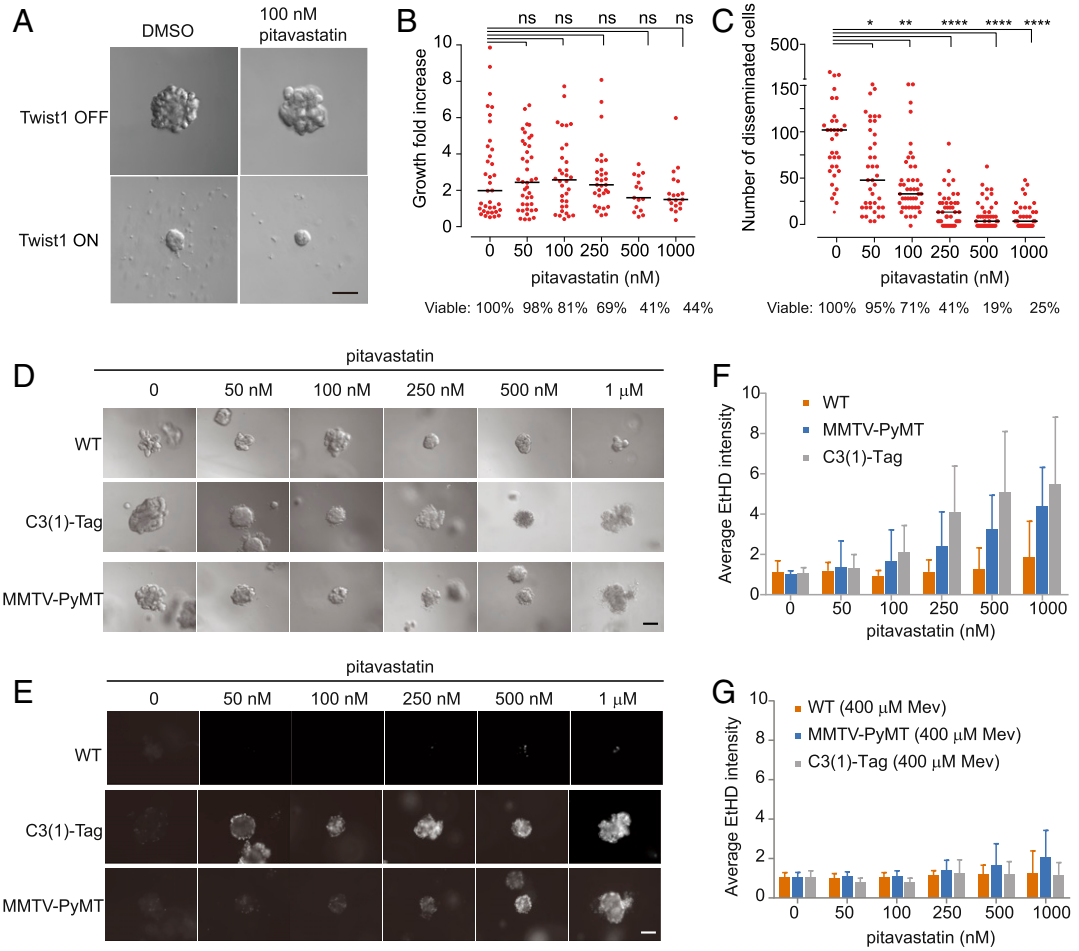

Fig. 8. Twist1 ON and tumor organoids in the mouse model exhibit vulnerability to pitavastatin. (*A*) Effects of pitavastatin on Twist1 ON organoids. (Scale bar, 100 μm.) (*B*) Measurement of the growth of Twist1 OFF organoids in response to increasing concentrations of pitavastatin ($n = 3$ experiments, nonparametric Mann–Whitney–Wilcoxon test). (*C*) Measurement of the disseminated cells of Twist1 ON organoids in response to increasing concentrations of pitavastatin ($n = 3$ experiments, nonparametric Mann–Whitney–Wilcoxon test, $^*P < 0.05$, $^{**}P < 0.01$, $^{***}P < 0.001$, $^{****}P < 0.0001$). (*D*) Effects of pitavastatin on viability of WT, C3 (1)-TAg, and MMTV-PyMT organoids. (Scale bar, 100 μm.) (*E*) Effects of pitavastatin on the viability of WT, C3 (1)-TAg, and MMTV-PyMT organoids. Dead cells are stained with ethidium homodimer (EthD). (Scale bar, 100 μm.) (*F*) Measurement of the cell death of tumor organoids in response to increasing concentrations of pitavastatin. (*G*) Measurement of the cell death of tumor organoids in the presence of 400 μM Mev and increasing concentrations of pitavastatin (mean ± SD, $n = 3$ experiments).

organoids (Twist1 ON), C3 (1)-TAg basal mammary tumors, and MMTV-PyMT luminal mammary tumors.

Expression of the EMT transcription factor Twist1 induces rapid dissemination in 3D organoids (33). As shown in Fig. 8 *A* and *B*, growth of Twist1 OFF organoids was unaffected with increasing doses of pitavastatin. In Twist1 ON organoids, pitavastatin caused a substantial reduction of dissemination and viability in a dose-dependent manner (Fig. 8 *A* and *C*).

We next sought to test the effects of pitavastatin on a luminal mammary carcinoma model in which the mouse mammary tumor virus drives the expression of the polyomavirus middle T oncogene (MMTV-PyMT) (34), and a basal mammary carcinoma model carrying C3 (1) simian virus 40 large tumor antigen fusion gene [C3 (1)-TAg] (35). As shown in Fig. 8 *D* and *E*, under 3D culture conditions, cells within C3 (1)-TAg organoids started to die with 50 nM pitavastatin and most had died at 250 nM, while those in MMTV-PyMT organoids started to die with 100 nM pitavastatin and most had died at 500 nM. The majority of wild-type organoids remained alive with 1 μM pitavastatin. Thus, these tumor organoids are much more sensitive to pitavastatin than normal organoids. As shown in Fig. 8*G*, addition of mevalonic acid dramatically inhibited the effects of pitavastatin in 3D tumor organoids. These results show that cancers with genetic defects other than PTEN deficiencies are sensitive to inhibition of the mevalonate pathway.

Discussion

Our observations bring together previously isolated studies of the role of the mevalonate pathway and macropinocytosis in cancer (Fig. 6*H*). On the one hand, the mevalonate pathway has been implicated in multiple aspects of tumorigenesis including controlling cell proliferation, survival, invasion, and metastasis (20, 36, 37). On the other hand, recent studies have suggested that macropinocytosis represents an important route of tumor nutrient uptake (21, 22). We demonstrate that statins target PTEN-deleted and Ras^{G12V}-expressing cells by selectively reducing macropinocytosis, which eventually leads to amino acid starvation and subsequent cell death. We traced the decreased macropinocytosis to depletion of GGPP rather than any other intermediate metabolites in the mevalonate pathway. These mechanisms hold for *Dictyostelium* amoebae and human epithelial cells. Consistently, *Dictyostelium ggps1*$^-$ cells showed defects in both cell motility and fluid-phase uptake before they died. By demonstrating that GGPP supports cell motility and macropinocytosis, we

explain why cells carrying oncogenic mutations, which have altered migration and nutrient uptake, are dependent on the mevalonate pathway.

Extensive studies have shown that a signal transduction network involving Ras GTPases and phosphoinositides is important in controlling cell morphological changes, and this is likely the reason why macropinocytosis in cells with oncogenic defects displays greater sensitivity to pitavastatin. First, the smaller, less intense macropinosomes in cells lacking PTEN are consistent with previous observations of actin-based protrusions in *Dictyostelium* (38). Lampert et al. showed that *pten*$^-$ cells display multidirected, smaller $LimE_{\Delta coil}$-RFP (a biosensor for newly formed F-actin)–positive patches on their membrane when compared with the wild-type cells. Furthermore, using electrofusion, a method developed to observe signaling and cytoskeletal traveling waves on the basal surface of cells, we found that electrofused *pten*$^-$ cells displayed smaller traveling waves on the basal surface. The traveling waves control the size of protrusions and most likely macropinosomes (8). The smaller waves have been interpreted in terms of excitable network theory, where increasing negative feedback reduces the wave range. PTEN deletion activates PKB, which provides negative feedback to Rap and Ras (4). We speculate that pitavastatin, by depleting GGPP needed for geranylgeranylation of Rap and certain Ras proteins, further decreases the excitability to a point where waves, protrusions, and macropinosomes rarely occur. Although we do not have direct evidence, the consistently defective macropinocytosis in both *Dictyostelium* and MCF10A cells might suggest that elevated PIP3 also provides negative feedback in mammalian cells. Second, in K-Ras^{G12V} cells, waves are generally larger and accordingly the macropinocytosis is increased. However, interference with geranylgeranylation also selectively inhibits macropinocytosis in these cells. We do not fully understand the mechanism in this case. Apparently, an optimal amount of Ras activity is most resistant to GGPP depletion. Another possibility might be related to a greater need for nutrients in K-Ras^{G12V}–expressing cells.

Our studies suggest that GGPP depletion kills cells by impairing macropinocytosis, leading to amino acid starvation. Furthermore, K-Ras^{G12V}–expressing cells may be even more sensitive to amino acid starvation than wild-type cells since K-Ras^{G12V} cells die sooner when we keep the medium unchanged for 96 h. While GGPP depletion could potentially lead to many defects in cells, loading pitavastatin-treated cells with additional protein mitigated cell death. Macropinocytosis is not restored to the level in control cells. This suggests that loading the residual macropinosomes with sufficient protein is critical rather than any other roles of GGPP.

Macropinocytosis itself is regulated by nutrient conditions and the regulation is complex (39, 40). On one hand, nutrient restriction can increase macropinocytosis. It has been reported that PTEN-deleted MEFs exhibit selectively induced macropinocytosis only with the activation of AMPK (glucose depletion), even though the mechanism is still unclear. With MCF10A cells, glucose or glutamine restriction and, as has been reported for other cell lines, serum starvation did increase macropinocytosis. However, these increases were not selective in PTEN-deleted cells. On the other hand, cells displayed induced macropinocytosis when we refreshed the medium 1 d before the uptake assay, indicating that nutrient availability can provide a positive effect on macropinocytosis. Thus, more studies are needed to further elucidate the connection between macropinocytosis and nutrient conditions.

Compared with inhibiting single geranylgeranylated proteins, depletion of GGPP was more efficient in targeting cancer cells. While previous studies suggested effects of the mevalonate pathway in cancer cells were mediated by RhoA (41, 42), in our hands, knocking down or overexpressing RhoA, or expressing a farnesylatable RhoA mutant, in MCF10A *PTEN*$^{-/-}$ cells minimally altered pitavastatin sensitivity. In addition, only slight effects were detected when individually overexpressing six of the eight GGTase-I target proteins in *Dictyostelium pten*$^-$ cells. In contrast, simultaneously expressing six of these proteins was able to partially suppress the effects of pitavastatin.

Our studies suggest that statins or GGPP synthase inhibitors should be examined as cancer therapeutics. We propose these drugs work by displacing a constellation of geranylgeranylated proteins needed for proper macropinocytosis. This process relies on a molecular network involving geranylgeranylated proteins as well as key oncogenes and tumor suppressors. Oncogenic mutations in cancer cells dysregulate the network and, when further insult occurs by blocking geranylgeranylation of multiple additional network components, macropinocytosis is inhibited. Since macropinocytosis is an important route for nutrient uptake, its reduction below a threshold level is unsustainable and the cells starve and die.

Methods

Dictyostelium discoideum cells, AX2, and *pten*$^-$ and *ggps1*$^-$ strains were cultured in HL5 medium or FM medium. Drug treatments were performed 30 min after seeding cells. For mammalian cells, MCF10A, *PTEN*$^{-/-}$, and K-Ras^{G12V}-GFP–expressing cells were cultured in 5% CO_2 in DMEM/F-12 high-glucose medium supplemented with horse serum, penicillin-streptomycin, EGF, hydrocortisone, cholera toxin, and insulin at 37 °C. Drug treatments were conducted 24 to 48 h after seeding cells. Macropinocytosis was performed as previously described (21). A detailed description of materials and methods is provided in *SI Appendix, Materials and Methods*.

Data Availability. All of the data in this study are included in the article or *SI Appendix*.

ACKNOWLEDGMENTS. We thank all members of the P.N.D. laboratories as well as members of the Iglesias, Iijima, and Robinson laboratories (Johns Hopkins University) for helpful suggestions. We thank the Jun Liu lab for providing the drug library. We thank F. Tamanoi for providing GGTI inhibitors, and D. Weimer for providing DGBP and advice. We thank S. Martin and M. Vitolo for providing the original *PTEN*$^{-/-}$ cells. We thank Zhenyu Zhang for protein sequence analysis. This work was supported by NIH Grant R35 GM118177 (to P.N.D.), Air Force Office of Scientific Research (AFOSR) Multidisciplinary Research Program of the University Research Initiative (MURI) FA95501610052, Defense Advanced Research Projects Agency (DARPA) HR0011-16-C-0139, as well as NIH Grant S10 OD016374 (to S. Kuo of the Johns Hopkins University Microscope Facility). A.J.E. received support for this project through grants from the Breast Cancer Research Foundation (BCRF-18-048) and the NIH/National Cancer Institute (U01CA217846, 3P30CA006973).

1. K. M. Yamada, M. Araki, Tumor suppressor PTEN: Modulator of cell signaling, growth, migration and apoptosis. *J. Cell Sci.* **114**, 2375–2382 (2001).
2. E. Castellano *et al.*, RAS signalling through PI3-kinase controls cell migration via modulation of Reelin expression. *Nat. Commun.* **7**, 11245 (2016).
3. X. Li *et al.*, Mutually inhibitory Ras-PI(3,4)P_2 feedback loops mediate cell migration. *Proc. Natl. Acad. Sci. U.S.A.* **115**, E9125–E9134 (2018).
4. Y. Miao *et al.*, Altering the threshold of an excitable signal transduction network changes cell migratory modes. *Nat. Cell Biol.* **19**, 329–340 (2017).
5. G. Gerisch *et al.*, Membrane and actin reorganization in electropulse-induced cell fusion. *J. Cell Sci.* **126**, 2069–2078 (2013).
6. C. H. Huang, M. Tang, C. Shi, P. A. Iglesias, P. N. Devreotes, An excitable signal integrator couples to an idling cytoskeletal oscillator to drive cell migration. *Nat. Cell Biol.* **15**, 1307–1316 (2013).
7. M. Tang *et al.*, Evolutionarily conserved coupling of adaptive and excitable networks mediates eukaryotic chemotaxis. *Nat. Commun.* **5**, 5175 (2014).
8. Y. Miao *et al.*, Wave patterns organize cellular protrusions and control cortical dynamics. *Mol. Syst. Biol.* **15**, e8585 (2019).
9. M. J. Wang, Y. Artemenko, W. J. Cai, P. A. Iglesias, P. N. Devreotes, The directional response of chemotactic cells depends on a balance between cytoskeletal architecture and the external gradient. *Cell Rep.* **9**, 1110–1121 (2014).
10. J. M. Yang *et al.*, Integrating chemical and mechanical signals through dynamic coupling between cellular protrusions and pulsed ERK activation. *Nat. Commun.* **9**, 4673 (2018).
11. S. Kawata *et al.*, Effect of pravastatin on survival in patients with advanced hepatocellular carcinoma. A randomized controlled trial. *Br. J. Cancer* **84**, 886–891 (2001).
12. W. S. Kim *et al.*, Phase II study of high-dose lovastatin in patients with advanced gastric adenocarcinoma. *Invest. New Drugs* **19**, 81–83 (2001).
13. J. J. Knox *et al.*, A phase I trial of prolonged administration of lovastatin in patients with recurrent or metastatic squamous cell carcinoma of the head and neck or of the cervix. *Eur. J. Cancer* **41**, 523–530 (2005).

14. J. Larner *et al*., A phase I-II trial of lovastatin for anaplastic astrocytoma and glioblastoma multiforme. *Am. J. Clin. Oncol.* **21**, 579–583 (1998).
15. M. D. Minden, J. Dimitroulakos, D. Nohynek, L. Z. Penn, Lovastatin induced control of blast cell growth in an elderly patient with acute myeloblastic leukemia. *Leuk. Lymphoma* **40**, 659–662 (2001).
16. A. Thibault *et al*., Phase I study of lovastatin, an inhibitor of the mevalonate pathway, in patients with cancer. *Clin. Cancer Res.* **2**, 483–491 (1996).
17. Y. G. Shellman *et al*., Lovastatin-induced apoptosis in human melanoma cell lines. *Melanoma Res.* **15**, 83–89 (2005).
18. M. Koyuturk, M. Ersoz, N. Altiok, Simvastatin induces proliferation inhibition and apoptosis in C6 glioma cells via c-jun N-terminal kinase. *Neurosci. Lett.* **370**, 212–217 (2004).
19. R. Girgert, Y. Vogt, D. Becke, G. Bruchelt, P. Schweizer, Growth inhibition of neuroblastoma cells by lovastatin and L-ascorbic acid is based on different mechanisms. *Cancer Lett.* **137**, 167–172 (1999).
20. W. A. Freed-Pastor *et al*., Mutant p53 disrupts mammary tissue architecture via the mevalonate pathway. *Cell* **148**, 244–258 (2012).
21. C. Commisso *et al*., Macropinocytosis of protein is an amino acid supply route in Ras-transformed cells. *Nature* **497**, 633–637 (2013).
22. W. Palm *et al*., The utilization of extracellular proteins as nutrients is suppressed by mTORC1. *Cell* **162**, 259–270 (2015).
23. G. Bloomfield *et al*., Neurofibromin controls macropinocytosis and phagocytosis in *Dictyostelium*. *eLife* **4**, e04940 (2015).
24. E. Holm *et al*., Substrate balances across colonic carcinomas in humans. *Cancer Res.* **55**, 1373–1378 (1995).
25. D. Gaglio, C. Soldati, M. Vanoni, L. Alberghina, F. Chiaradonna, Glutamine deprivation induces abortive S-phase rescued by deoxyribonucleotides in K-Ras transformed fibroblasts. *PLoS One* **4**, e4715 (2009).
26. O. Larsson, HMG-CoA reductase inhibitors: Role in normal and malignant cells. *Crit. Rev. Oncol. Hematol.* **22**, 197–212 (1996).
27. T. Ugawa *et al*., YM-53601, a novel squalene synthase inhibitor, reduces plasma cholesterol and triglyceride levels in several animal species. *Br. J. Pharmacol.* **131**, 63–70 (2000).
28. E. C. Lerner *et al*., Ras CAAX peptidomimetic FTI-277 selectively blocks oncogenic Ras signaling by inducing cytoplasmic accumulation of inactive Ras-Raf complexes. *J. Biol. Chem.* **270**, 26802–26806 (1995).
29. A. Vogt, J. Sun, Y. Qian, A. D. Hamilton, S. M. Sebti, The geranylgeranyltransferase-I inhibitor GGTI-298 arrests human tumor cells in G0/G1 and induces p21(WAF1/CIP1/SDI1) in a p53-independent manner. *J. Biol. Chem.* **272**, 27224–27229 (1997).
30. T. Kainou, K. Kawamura, K. Tanaka, H. Matsuda, M. Kawamukai, Identification of the GGPS1 genes encoding geranylgeranyl diphosphate synthases from mouse and human. *Biochim. Biophys. Acta* **1437**, 333–340 (1999).
31. N. Mizushima, T. Yoshimori, B. Levine, Methods in mammalian autophagy research. *Cell* **140**, 313–326 (2010).
32. W. W. Wong, J. Dimitroulakos, M. D. Minden, L. Z. Penn, HMG-CoA reductase inhibitors and the malignant cell: The statin family of drugs as triggers of tumor-specific apoptosis. *Leukemia* **16**, 508–519 (2002).
33. E. R. Shamir *et al*., Twist1-induced dissemination preserves epithelial identity and requires E-cadherin. *J. Cell Biol.* **204**, 839–856 (2014).
34. C. T. Guy, R. D. Cardiff, W. J. Muller, Induction of mammary tumors by expression of polyomavirus middle T oncogene: A transgenic mouse model for metastatic disease. *Mol. Cell. Biol.* **12**, 954–961 (1992).
35. I. G. Maroulakou, M. Anver, L. Garrett, J. E. Green, Prostate and mammary adenocarcinoma in transgenic mice carrying a rat C3(1) simian virus 40 large tumor antigen fusion gene. *Proc. Natl. Acad. Sci. U.S.A.* **91**, 11236–11240 (1994).
36. J. W. Clendening *et al*., Dysregulation of the mevalonate pathway promotes transformation. *Proc. Natl. Acad. Sci. U.S.A.* **107**, 15051–15056 (2010).
37. M. Koyuturk, M. Ersoz, N. Altiok, Simvastatin induces apoptosis in human breast cancer cells: p53 and estrogen receptor independent pathway requiring signalling through JNK. *Cancer Lett.* **250**, 220–228 (2007).
38. T. J. Lampert *et al*., Shear force-based genetic screen reveals negative regulators of cell adhesion and protrusive activity. *Proc. Natl. Acad. Sci. U.S.A.* **114**, E7727–E7736 (2017).
39. J. A. Swanson, C. Watts, Macropinocytosis. *Trends Cell Biol.* **5**, 424–428 (1995).
40. J. A. Swanson, Shaping cups into phagosomes and macropinosomes. *Nat. Rev. Mol. Cell Biol.* **9**, 639–649 (2008).
41. E. Ingallina *et al*., Mechanical cues control mutant p53 stability through a mevalonate-RhoA axis. *Nat. Cell Biol.* **20**, 28–35 (2018).
42. G. Sorrentino *et al*., Metabolic control of YAP and TAZ by the mevalonate pathway. *Nat. Cell Biol.* **16**, 357–366 (2014).